Journal of Porphyrins and Phthalocyanines
J. Porphyrins Phthalocyanines 2013; **17**: 1–13
DOI: 10.1142/S1088424613500557

Published at http://www.worldscinet.com/jpp/

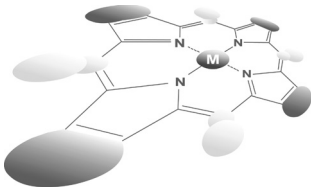

Synthesis, structural characterization and protonation/deprotonation of hydroxyl-substituted free-base tetraphenylporphyrins in nonaqueous media

Guifen Lu[a◊◊], Xiufeng Zhang[a], Xu Cai[a], Yuanyuan Fang[b], Min Zhu[a], Weihua Zhu[a], Zhongping Ou*[a◊] and Karl M. Kadish*[b◊]

[a] *School of Chemistry and Chemical Engineering, Jiangsu University, Zhenjiang 212013, P. R. China*
[b] *Department of Chemistry, University of Houston, Houston, TX 77204-5003, USA*

Dedicated to Professor Vefa Ahsen on the occasion of his 60th birthday

Received 18 March 2013
Accepted 11 April 2013

ABSTRACT: A series of hydroxyl-substituted free-base tetraphenylporphyrins was synthesized and characterized by UV-vis spectroscopy, ^{1}H NMR and mass spectrometry. The porphyrins are represented as $(HOPh)_n(t\text{BuPh})_{4-n}PH_2$, where Ph presents a phenyl group, HO and *t*Bu are substituents on the para-positions of the phenyl rings of the macrocycle, n = 0–4 and P represents the dianion of tetraphenylporphyrin. The UV-visible properties of each porphyrin were examined in dichloromethane (DCM), *N*,*N*′-dimethylformamide (DMF) and dimethyl sulfoxide (DMSO) before and after addition of trifluoroacetic acid (TFA) or sodium hydroxide (NaOH) to solution. Equilibrium constants for protonation ($\log\beta_n$) and deprotonation ($\log\beta'_n$) of each compound were determined using standard equations. The protonations occur in a single step involving a simultaneous two proton addition at the porphyrin central nitrogens. The phenolic protons on $(HOPh)_n(t\text{BuPh})_{4-n}PH_2$ are easier to deprotonate than the core nitrogen protons of the porphyrins and this reaction occurs in a single step involving the simultaneous loss of 1–4 protons on the hydroxyl groups followed by a loss of two protons from the central nitrogens. The effect of HO substituents on UV-visible spectra and the magnitude of the protonation/deprotonation constants ($\log\beta_n$ and $\log\beta'_n$) are discussed. Two of the porphyrins, $(t\text{BuPh})_4PH_2$ and *trans*-$(HOPh)_2(t\text{BuPh})_2PH_2$, are also characterized by a single-crystal X-ray analysis.

KEYWORDS: hydroxyl-substituted free-base porphyrins, UV-vis spectra, protonation and deprotonation, crystal structures.

INTRODUCTION

Free-base porphyrins have attracted a great deal of interest, in part because of their spectral and electrochemical properties [1–6] and in part because these compounds can be utilized in a variety of biomedical applications [7–10]. It is well-known that free-base porphyrins can be protonated and deprotonated, either in aqueous or nonaqueous media [11–14]. The gain or loss of protons on these molecules is accompanied by substantial changes in their spectroscopic properties, thus potentially making them either more or less effective in a variety of applications [15–17].

Our recent research interest has focused in part on protonated and deprotonated free-base porphyrins [18] and corroles [19–21] containing different electron-donating or electron-withdrawing substituents on the macrocycle. In the present work, we have expanded upon our work in this area to include a newly synthesized series of phenol-substituted free-base tetraphenylporphyrins

[◊] SPP full and [◊◊] student member in good standing

*Correspondence to: Zhongping Ou, email: zpou2003@yahoo.com, tel/fax: +86 511-8879-1800; Karl M. Kadish, email: kkadish@uh.edu, tel: +1 (713)-743-2740, fax: +1 (713)-743-2745

where the HO groups can act not only as strongly electron-withdrawing substituents on the tetraphenylporphyrin macrocycle, but can also be deprotonated in nonaqueous media containing added acid. The investigated compounds are shown in Chart 1 and are represented as $(HOPh)_n(t\text{BuPh})_{4-n}PH_2$, where Ph presents a phenyl group, HO and *t*Bu are substituents on *para*-position of the *meso* phenyl rings of the macrocycle, $n = 0$, 1, 2, 3, and 4 and P is a dianion of tetraphenylporphyrin.

Examination of the spectral properties for phenol-substituted free-base porphyrins has atracted more interests because these compounds have potential applications in the photodynamic therapy of cancer [22]. However, to our knowledge, there have been no systematic examination of the spectroscopic and acid/base properties so far for these kinds of compounds, and this is done in the present paper where the porphyrins in Chart 1 were examined as to their UV-visible spectral properties in dichloromethane (DCM), *N*,*N*′-dimethylformamide (DMF) and dimethyl sulfoxide (DMSO) before and after addition of TFA and NaOH to solution.

Each protonated and deprotonated free-base porphyrin was spectroscopically characterized and the progress of the acid or base titrations was monitored by UV-visible spectroscopy, enabling calculation of both protonation and deprotonation constants using standard equations. The UV-visible spectra and protonation/deprotonation constants for the series of hydroxylated porphyrins are discussed in terms of the specific nonaqueous solvent and number of HO groups on the macrocycle.

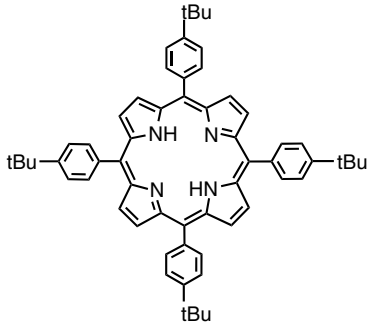

$(t\text{BuPh})_4PH_2$ **1**

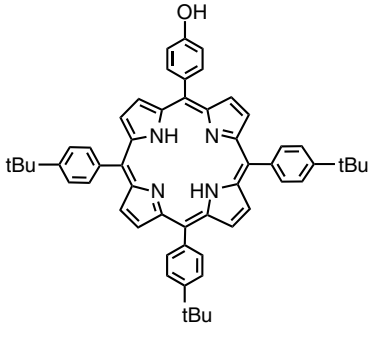

$(HOPh)(t\text{BuPh})_3PH_2$ **2**

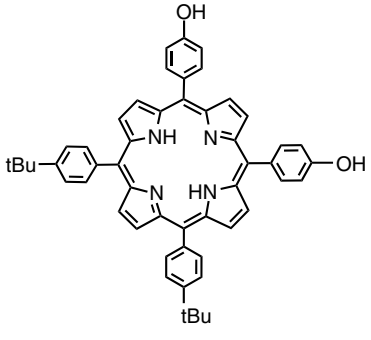

cis-$(HOPh)_2(t\text{BuPh})_2PH_2$ **3**

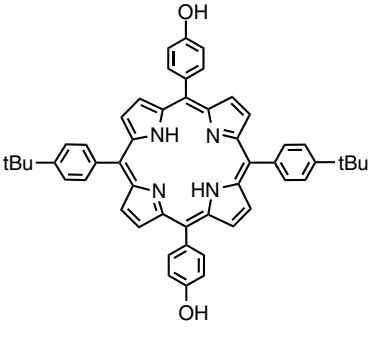

trans-$(HOPh)_2(t\text{BuPh})_2PH_2$ **4**

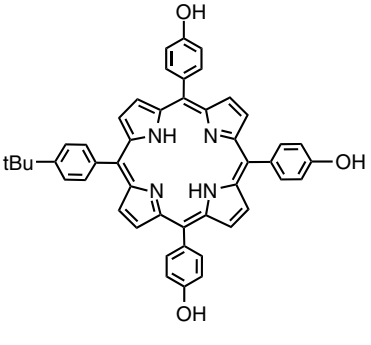

$(HOPh)_3(t\text{BuPh})PH_2$ **5**

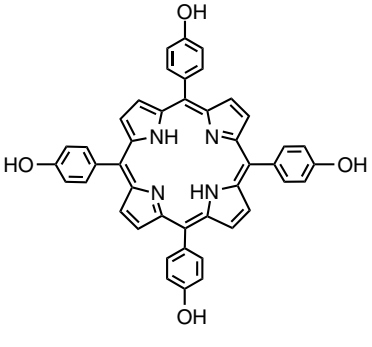

$(HOPh)_4PH_2$ **6**

Chart 1. Structures of the investigated free-base porphyrins

EXPERIMENTAL

Materials and equipment

N,*N*′-dimethylformamide and dichloromethane were distilled over P_2O_5 and pyrrole was distilled over CaH_2 under vacuum prior to use. TFA (99+%) and DMSO were purchased from Sigma-Aldrich Chemical Co. All other chemicals are analytical grade and used as received. Column chromatography was carried out on silica gel (Merck, Kieselgel 60, 70-230 mesh) with the given eluent.

UV-visible spectra were measured with an Agilent 8453 diode array spectrophotometer. ^{1}H NMR spectrum was measured on a Bruker DPX 300 spectrometer (300 MHz) in $CDCl_3$ and DMSO-d_6. MALDI-TOF mass spectrum was recorded on a Bruker BIFLEX III ultrahigh resolution with α-cyano-4-hydroxycinnamic acid as matrix. Elemental analysis was performed on an Elementar Vavio El III.

Synthesis

The free-base porphyrins were prepared according to methods described in the literature [23–25]. Freshly distilled pyrrole (5.5 mL, 80 mmol) was added over a period of 15 min to a solution of *tert*-butyl benzaldehyde, 4-hydroxybenzaldehyde and propionic acid (200 mL) at 140 °C. The solution was then refluxed for 30 min, cooled and left overnight at -5 °C, and then filtered at reduced pressure to give a dark purple powder. The crude porphyrins were eluted on a silica gel column using methanol/chloroform as eluent. The amount of the main reactants utilized (pyrrole, *tert*-butyl benzaldehyde and 4-hydroxybenzaldehyde) and the yield of each isolated porphyrin are shown in Table 1.

(*t*BuPh)$_4$PH$_2$ 1. ^{1}H NMR ($CDCl_3$): δ, ppm -2.70 (s, 2H), 1.64 (s, 36H), 7.79 (d, 8H), 8.18 (d, 8H) and 8.90 (s, 8H). MALDI-TOF mass: *m/z* $C_{60}H_{62}N_4$, calcd. 839.2, found 840.7.

(HOPh)(*t*BuPh)$_3$PH$_2$ 2. ^{1}H NMR ($CDCl_3$): δ, ppm -2.71 (s, 2H), 1.64 (s, 9H), 7.12 (d, 2H), 7.78 (d, 6H), 8.07 (d, 2H), 8.18 (d, 6H) and 8.88 (t, 8H). MALDI-TOF mass: *m/z* $C_{56}H_{54}N_4O$, calcd. 799.1, found 800.7.

***cis*-(HOPh)$_2$(*t*BuPh)$_2$PH$_2$ 3.** Anal. calcd. (%) for $C_{52}H_{46}N_4O_2$: C, 82.29; H, 6.11; N, 7.38. Found (%): C, 82.05; H, 6.24; N, 7.26. ^{1}H NMR (DMSO-d_6): δ, ppm -2.89 (s, 2H), 1.57 (s, 18H), 7.22 (d, 4H), 7.84 (d, 4H), 8.02 (d, 4H), 8.14 (d, 4H), 8.82 (t, 4H), 8.88 (s, 4H) and 9.96 (s, 2H). MALDI-TOF mass: *m/z* calcd. 759.0, found 759.7.

(HOPh)$_3$(*t*BuPh)PH$_2$ 5. Anal. calcd. (%) for $C_{48}H_{38}N_4O_3$: C, 80.20; H, 5.33; N, 7.79. Found (%): C, 80.09; H, 5.41; N, 7.68. ^{1}H NMR (DMSO-d_6): δ, ppm -2.89 (s, 2H), 1.58 (s, 9H), 7.22 (d, 6H), 7.86 (d, 2H), 8.01 (d, 6H), 8.16 (d, 2H), 8.81 (d, 2H), 8.87 (s, 6H) and 9.96 (s, 3H). MALDI-TOF mass: *m/z* calcd. 718.8, found 719.5.

(HOPh)$_4$PH$_2$ 6. ^{1}H NMR (DMSO-d_6): δ, ppm -2.88 (s, 2H), 7.22 (d, 8H), 8.01 (d, 8H), 8.87 (s, 8H) and 9.96 (s, 4H). MALDI-TOF mass: *m/z* $C_{44}H_{30}N_4O_4$, calcd. 678.7, found 679.1.

***trans*-(HOPh)$_2$(*t*BuPh)$_2$PH$_2$ 4.** The yield of **4** was very low (see Table 1) with the Alder–Longo synthetic method [22, 23] and a modified synthetic route of Lindsey and coworkers [28] was followed. The synthetic procedure is shown in Scheme 1 and described below.

Pyrrole (30 mL, 0.45 mol) and *tert*-butyl benzaldehyde (2.5 mL, 0.015 mol) were mixed and degassed with N_2 for 5 min. After addition of TFA (100 μL, 1.5 mmol), the solution was stirred under N_2 at room temperature for 5 min and then quenched with K_2CO_3. The reaction mixture was filtered and eluted with acetic ester. The filtrate was collected and the solvent removed under vacuum to give a gray solid. Purification of the crude product by column chromatography (silica gel, petroleum:ether-acetic ester = 3:1) afforded a light gray product, 5-(4-*tert*-butylphenyl)dipyrromethane (3.97 g, 95%). ^{1}H NMR ($CDCl_3$, ppm): 1.29 (s, 9H), 5.43 (s, 1H), 5.93 (m, 2H), 6.16 (t, 2H), 6.67 (m, 2H), 7.14 (d, 2H), 7.33 (d, 2H), 7.87 (s, br, 2H).

A mixture of 5-(4-*tert*-butylphenyl)dipyrromethane (2.78 g, 10 mmol), 4-hydroxybenzaldehyde (1.22 g, 10 mmol) and ammonium chloride (1.69 g, 30 mmol) in DMSO (100 mL) was heated at 90 °C for 24 h and then cooled to room temperature. The crude reaction mixture was filtered and the solid then purified by column

Table 1. Amount of the main reactants (mmol) and yield (%) of the free-base porphyrins

Compound	Pyrrole, mmol	*tert*-butyl benzaldehyde, mmol	4-hydroxy benzaldehyde, mmol	Yield, %
(*t*BuPh)$_4$PH$_2$ **1**	80	80	0	40
(HOPh)(*t*BuPh)$_3$PH$_2$ **2**	80	20	60	30
cis-(HOPh)$_2$(*t*BuPh)$_2$PH$_2$ **3**	80	40	40	15
trans-(HOPh)$_2$(*t*BuPh)$_2$PH$_2$ **4**	80	40	40	0.2
(HOPh)$_3$(*t*BuPh)PH$_2$ **5**	80	60	20	10
(HOPh)$_4$PH$_2$ **6**	80	0	80	7

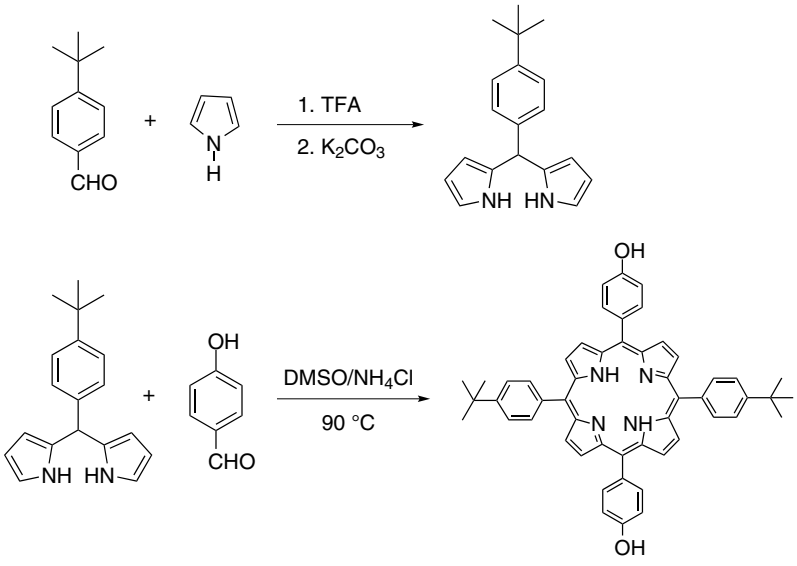

Scheme 1. Synthesis route for the preparation of *trans*-$(HOPh)_2(t\text{BuPh})_2PH_2$ **4**

chromatography (silica gel, chloroform). After removal of the solvent and drying under vacuum the purple solid of *trans*-$(HOPh)_2(t\text{BuPh})_2PH_2$ **4** was obtained. Yield 5%. Anal. calcd. (%) for $C_{52}H_{46}N_4O_2$: C, 82.29; H, 6.11; N, 7.38. Found (%): C, 82.39; H, 6.12; N, 6.96. MALDI-TOF mass: *m/z* calcd. 759.0, found 759.1. ^{1}H NMR (DMSO-d_6): δ, ppm -2.90 (s, 2H), 1.59 (s, 18H), 8.17 (d, 4H), 8.01 (d, 4H), 7.87 (d, 4H), 7.22 (d, 4H), 8.89 (d, 4H), 8.82 (d, 4H) and 9.96 (s, 2H).

X-ray crystallography

Single crystals of $(t\text{BuPh})_4PH_2$ **1** and *trans*-$(HOPh)_2(t\text{BuPh})_2PH_2$ **4** for X-ray diffraction analysis were obtained by slow diffusion of methanol into toluene and chloroform solutions, respectively. The crystals were mounted on a glass fiber and the crystal data were collected on a Bruker SMART APEXII CCD diffractometer with graphite monochromatic Mo Ka radiation (λ = 0.71073 Å) using a ω scan mode at 293 K. The crystal structure was solved by direct methods (SHELXS-97) and refined by fullmatrix least-squares (SHELXL-97) on F^2. The non-hydrogen atoms were refined anisotropically and hydrogen atoms were added according to theoretical models. Intensity data were corrected for factors and empirical absorption.

Determination of equilibrium constants

A series of TFA/DCM, TFA/DMF or TFA/DMSO mixed solvents containing different concentrations of TFA was prepared and used as the acid-titration reagent. The base-titration reagent was NaOH solution (1.2×10^{-6} -1.2 M). In order to study the spectral changes *in situ*, micro-liter quantities of the above standard solutions were added gradually to a 5.5 mL DCM, DMF or DMSO solution of the porphyrin in a home-made 1.0 cm cell. After each addition of acid or base, the solution was thoroughly mixed and the spectrum recorded. The changes in spectra were analyzed as a function of the concentration of added acid or added base and the Hill equation was used to calculate the equilibrium constants, $\log\beta_n$ and $\log\beta'_n$, as described in the literature [19, 20, 26, 27]. Equilibrium constants were measured at room temperature (298 K).

RESULTS AND DISCUSSION

Synthesis and characterization

The investigated porphyrins possessed zero, one, two, three and four hydroxyl substituents on the *para*-positions of the *meso*-phenyl rings and *tert*-butyl groups at the *para*-positions lacking an HO group. The use of *tert*-butyl phenyl groups was to give the porphyrins increased solubility in common organic solvents such as chloroform, DCM and DMF. The difference in polarity between the *tert*-butyl and hydroxyl substituents on the compounds also enabled the hydroxylated porphyrins in the series to be more easily separated and purified.

As seen in Table 1, a relative good yield was obtained for compounds **1–3**, **5** and **6** when the Alder–Longo method was utilized. However, this was not the case for compound **4**, where the yield was only 0.2% by the same method. This compound was therefore synthesized by condensation of 5-(4-*tert*-butylphenyl)-dipyrromethane and 4-hydroxybenzaldehyde in the presence of an NH_4Cl catalyst [28] and was obtained with a higher yield of 5%.

The MALDI-TOF mass spectrum of each compound clearly shows an intense signal for the molecular ion $[M]^+$. Well-resolved ^{1}H NMR spectra are observed in DMSO-d_6 and the peak assignments could easily be

reached on the basis of integration and multiplicity of the signals.

X-ray single crystal structure

The crystal and molecular structures of (tBuPh)$_4$PH$_2$ **1** and *trans*-(HOPh)$_2$(tBuPh)$_2$PH$_2$ **4** were determined by X-ray diffraction analyses. The crystal data are summarized in Table 2 and the molecular structures are shown in Fig. 1. Both compounds **1** and **4** crystallize in the monoclinic system with $P2_1/c$ space group.

Compounds **1** and **4** have four identical substituents on the *meso*-positions of the porphyrin macrocycle and exhibit C_{2v} asymmetry. The four *meso*-phenyl rings are neither parallel nor perpendicular with the conjugated porphyrin π system and the dihedral angles between the phenyl substituent and the porphyrin mean plane are 61.8 and 70.4° for **1** and 62.3 and 80.6° for **4** due to the steric effect. It is worth noting that crystal packing of the porphyrin molecules in **1** and **4** are different from each other because of the different peripheral substituents and solvent molecules in the crystal.

For compound **1**, the neighboring molecules exhibit intermolecular C-H···π bonds between the phenyl hydrogen atom and porphyrin core, giving a three-dimensional supramolecular packing mode. However, there are two methanol molecules in the crystal structure of **4** and the neighboring molecules in **4** are connected by hydrogen bonds. As seen in Fig. 2, methanol molecules are located in the cavity of the crystals and are involved in hydrogen bonding within the superstructure; this differs from what was observed for 5,10,15,20-tetrakis(3,5-dimethyl-4-hydroxyphenyl)porphyrin [29].

There are two kinds of H-bonding in this network. One is between the imine nitrogen (N_1) and methanol hydrogen (H_3) [O_3–H_3····$N_{1:}$ = 2.948(4) Å, ∠$O_3H_3N_1$ = 167.5°, symmetry code: x, -y + 1/2, z + 1/2]. The other is between the phenolic hydrogen (H_1) and the methanol oxygen (O_3) [O_1–H_1····O_3: = 2.693(3) Å, ∠$O_1H_1O_3$ = 172.4°, symmetry code: -x + 2, -y, -z + 1]. The cooperation between these two kinds of hydrogen bonding leads to a comparatively complicated three-dimensional supramolecular structure (Fig. S1).

UV-vis spectral properties

Previously characterized 4-hydroxyphenyl substituents free-base porphyrins were shown to exhibit a single sharp

Table 2. Crystallographic data for (tBuPh)$_4$PH$_2$ (**1**) and *trans*-(HOPh)$_2$(tBuPh)$_2$PH$_2$ (**4**)

	1	**4**
Empirical formula	$C_{60}H_{62}N_4$	$C_{54}H_{54}N_4O_4$
Formula weight	839.14	823.01
Crystal size, mm	0.23 × 0.22 × 0.19	0.22 × 0.20 × 0.20
Crystal system	monoclinic	monoclinic
Space group	$P2_1/c$	$P2_1/c$
a, Å	13.637(3)	12.461(3)
b, Å	16.274(3)	15.818(3)
c, Å	11.482(2)	12.572(3)
Volume, A^3	2450.3(8)	2286.92
Z	2	2
F (000)	900	876
Calculated density, mg/m^3	1.137	1.195
Absorption coefficient, mm^{-1}	0.066	0.075
θ range (°) for data collection	3.11–25.33	3.12–25.34
Limiting indices	-13 ≤ h ≤ 16, -19 ≤ k ≤ 15, -12 ≤ l ≤ 13	-15 ≤ h ≤ 11, -15 ≤ k ≤ 19, -12 ≤ l ≤ 15
Reflections collected	11351	11513
Unique reflections [R(int)]	4439 [R(int) = 0.0581]	4134 [R(int) = 0.0524]
Completeness to θ = 25.34 (%)	99.1%	99.1%
Final R indices [I > 2(I)]	$R1$ = 0.0820, $wR2$ = 0.1698	$R1$ = 0.0826, $wR2$ = 0.2634
goodness of fit (GOF) on F^2	1.004	1.039
Largest diff. in peak and hole, e.A^{-3}	0.488 and -0.551	0.411 and -0.247

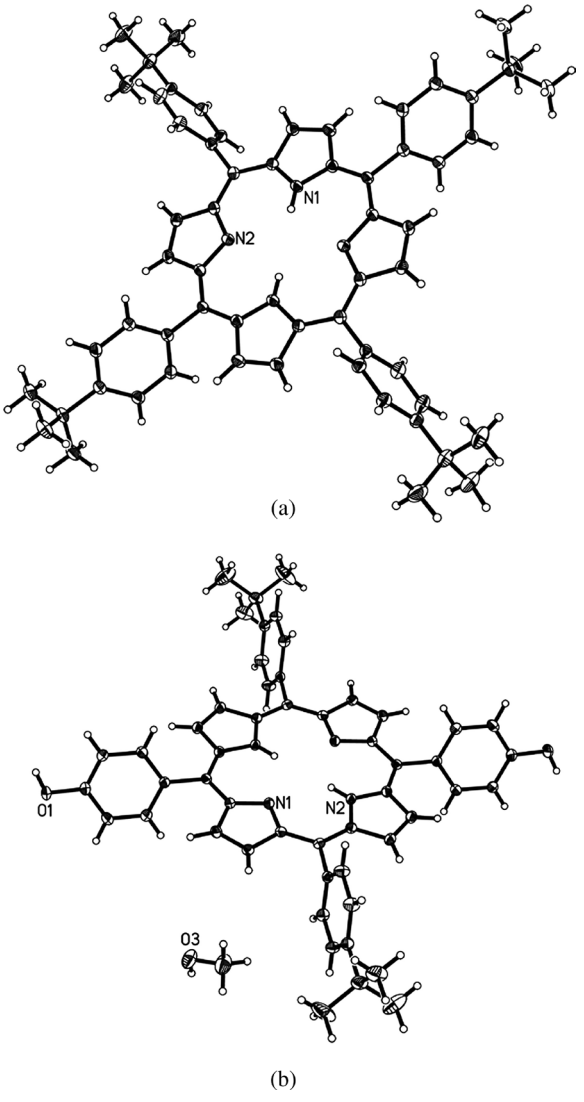

Fig. 1. Molecular structures of (a) (tBuPh)$_4$PH$_2$ **1** and (b) *trans*-(HOPh)$_2$(tBuPh)$_2$PH$_2$ **4** (showing 30% probability thermal displacement ellipsoids)

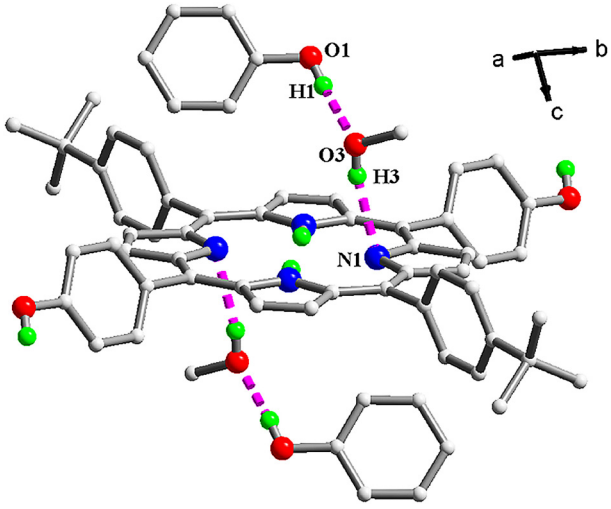

Fig. 2. Hydrogen-bonding manifold in *trans*-(HOPh)$_2$(tBuPh)$_2$-PH$_2$ **4** involves all of its phenolic protons, the core nitrogen atoms and the methanol molecules. Important bond lengths and angles: O1-O3, 2.693(3) Å; O3-N1, 2.948(4) Å; ∠O1-H1-O3, 172.4°; ∠O3-H3-N1, 167.5°

Soret band and four Q-bands between 510 and 650 nm [30] and this is also the case for compounds **1–6** in DCM, DMF and DMSO. The spectra of each porphyrin in DCM (Table 3) are similar to each other in a given solvent, regardless of the number and position of the hydroxyl groups. This is not the case in DMF and DMSO where the Soret and Q-bands dependent upon the number of HO groups and type of solvent as discussed later in the manuscript.

The addition of H^+ or OH^- to solutions of free-base porphyrins has been shown to result in significantly different UV-visible spectra [11–17]. This is also the case for the currently studied compounds. For example, in DMSO, neutral (HOPh)$_3$(tBuPh)PH$_2$ **5** has a Soret band at 424 nm and four Q-bands at 520, 557, 599 and 656 nm (Table 3). However, for the same compound in solutions of DMSO with added TFA, the Soret band is red-shifted to 458 nm and only one Q-band is observed at 702 nm. This change of the spectral properties is consistent with protonation of the porphyrin nitrogens under the given solution conditions. Different spectra are also seen for the deprotonated porphyrins as shown Fig. 3 which illustrated the UV-vis spectrum of compound **5** in its neutral, protonated and deprotonated forms. The

Table 3. UV-visible spectral data (λ_{max}, nm) in DCM, DMF and DMSO

Compound	In DCM		In DMF		In DMSO	
	Soret band	Q-bands	Soret band	Q-bands	Soret band	Q-bands
(tBuPh)$_4$PH$_2$ **1**	420	517, 553, 592, 645	419	517, 551, 595, 631	a	a
(HOPh)(tBuPh)$_3$PH$_2$ **2**	420	518, 554, 592, 645	420	517, 554, 594, 640	422	519, 556, 597, 651
cis-(HOPh)$_2$(tBuPh)$_2$PH$_2$ **3**	420	518, 553, 594, 647	421	517, 556, 594, 643	423	517, 553, 598, 652
trans-(HOPh)$_2$(tBuPh)$_2$PH$_2$ **4**	420	518, 553, 594, 649	421	516, 556, 596, 650	423	519, 555, 598, 650
(HOPh)$_3$(tBuPh)PH$_2$ **5**	420	519, 554, 594, 651	422	520, 557, 595, 652	424	520, 557, 599, 656
(HOPh)$_4$PH$_2$ **6**	a	a	423	519, 558, 597, 652	425	521, 560, 597, 655

[a] No data obtained due to the very limited solubility of the compound under the given solution conditions.

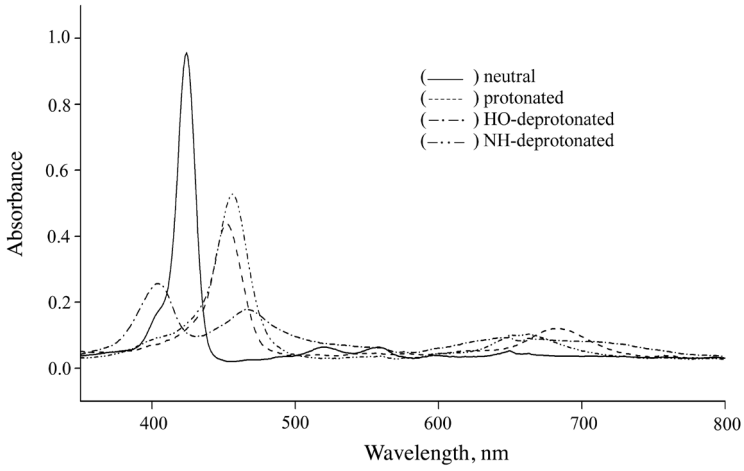

Fig. 3. UV-vis spectra of the neutral, protonated and deprotonated HO or NH forms of $(HOPh)_3(tBuPh)PH_2$ **5** in DMSO

protonation and deprotonation reactions are discussed in the following sections of the manuscript.

Protonation reactions

Figure 4 illustrates the UV-vis changes of $(HOPh)(tBuPh)_3PH_2$ **2** during a titration with TFA in DMF. As seen in this figure, the Soret band of the neutral porphyrin at 420 nm decreases in intensity while a new Soret band at 451 nm grows in for the diprotonated porphyrin. The number of Q-bands is also reduced from four (at 517, 554, 594 and 640 nm) to one (at 684 nm) as the protonated porphyrin is generated according to Equation 1.

$$(HOPh)(tBuPh)_3PH_2 + 2H^+ \rightleftharpoons [(HOPh)(tBuPh)_3PH_4]^{2+} \quad (1)$$

The spectral changes in Fig. 4 were analyzed as a function of the TFA concentration which enabled calculation of the number of protons added and the protonation constant ($\log\beta_n$) using the Hill equation [19, 20, 26, 27]. The diagnostic plot for analysis of the data at 415 nm is shown as an insert in Fig. 4 where a linear relationship is seen in the plot of $\log[(A_i-A_o)/(A_f-A_i)]$ *vs.* log[TFA]. The slope of the line is 2.0, indicating that two protons are added in a one-step process to give $[(HOPh)(tBuPh)_3PH_4]^{2+}$ as the final protonation product. A protonation constant of $\log\beta_2 = 4.7$ was then calculated from the zero intercept of the plot.

Similar changes in the UV-vis spectra were observed for the five other porphyrins when TFA was stepwise added to a DMF solution of the compound (Fig. S2). In each case the final products of titration exhibited a red shifted Soret band and a single Q-band at 673–710 nm. These types of spectral changes are typical for formation of a diprotonated porphyrinin nonaqueous media [11, 31].

The protonation reactions of compounds **1–6** was also investigated in DCM and DMSO and in each solvent two protons were again added in a single step ($n = 2.0$). Values of $\log\beta_2$ are given in Table 4 and ranged from 9.4 to 9.9 in DCM, from 3.3–5.4 in DMF and from 3.5–4.6 in DMSO, respectively.

Deprotonation reactions

The deprotonation reactions of **1–6** were examined by titration with NaOH in DMF and DMSO during addition of NaOH into solutions of the compound. Examples of the spectral changes are given in Figs 5–7 and a summary of the data is given in Table 5.

Compound **1** contains no hydroxyl groups and only the central NH groups of $(tBuPh)_4PH_2$ can be deprotonated. This reaction occurs in a single step with a loss of two protons as indicated by the slope of the Hill plot ($n = 2.0$) in Fig. 5. This result is consistent with results previously reported for the structurally related porphyrins $[(OCH_3)_3Ph]_4PH_2$ [31] and $(Ph)_4PH_2$ [32]. The prevailing

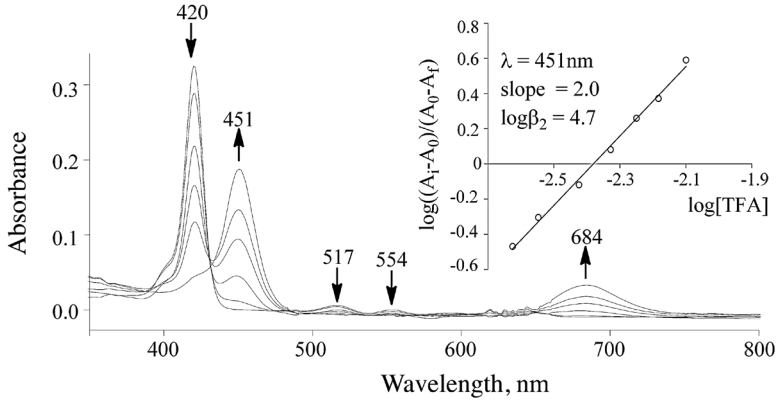

Fig. 4. UV-visible spectral changes of $(HOPh)(tBuPh)_3PH_2$ **2** in DMF during protonation of the central nitrogens by addition of TFA to solution. The insert shows the Hill plot used for calculation of the $\log\beta_2$

Table 4. UV-vis spectral data (λ_{max}, nm) of protonated free-base porphyrins and the protonation constants ($\log\beta_2$) in DCM, DMF and DMSO

Compound	In DCM				In DMF				In DMSO			
	Soret band	Q-band	*n*	$\log\beta_2$	Soret band	Q-band	*n*	$\log\beta_2$	Soret band	Q-band	*n*	$\log\beta_2$
(*t*BuPh)$_4$PH$_2$ **1**	445	670	2.0	9.9	447	673	2.0	3.3	a	a	a	a
(HOPh)(*t*BuPh)$_3$PH$_2$ **2**	445	672	2.0	9.7	451	684	2.0	4.7	451	692	2.0	3.5
cis-(HOPh)$_2$(*t*BuPh)$_2$PH$_2$ **3**	445	675	2.0	9.6	453	690	2.0	4.8	454	696	2.0	3.8
trans-(HOPh)$_2$(*t*BuPh)$_2$PH$_2$ **4**	445	675	2.0	9.6	454	692	2.0	5.1	456	697	2.0	4.0
(HOPh)$_3$(*t*BuPh)PH$_2$ **5**	447	680	2.0	9.4	455	699	2.0	5.2	458	702	2.0	4.4
(HOPh)$_4$PH$_2$ **6**	a	a	a	a	456	710	2.1	5.4	458	711	2.0	4.6

[a] No data obtained due to the very limited solubility of the compound under the given solution conditions.

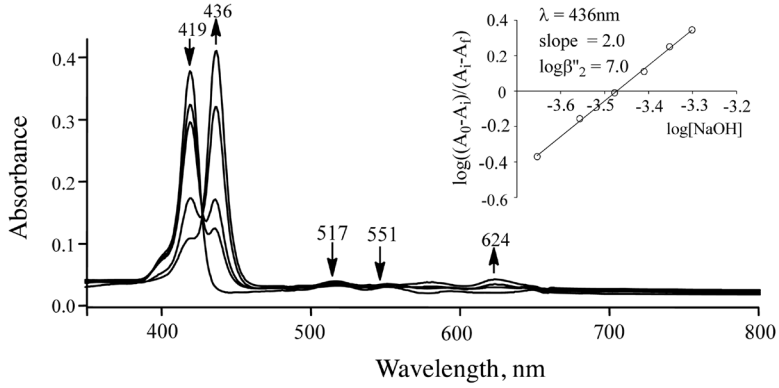

Fig. 5. UV-visible spectral changes of (*t*BuPh)$_4$PH$_2$ **1** during deprotonation by addition of NaOH in DMF

Table 5. Equilibrium constants ($\log\beta'_n$ and $\log\beta''_2$) for HO- and NH-deprotonation reactions of the free-base porphyrins in DMF and DMSO

Compound	In DMF					In DMSO				
	HO-deprotonation			NH-deprotonation		HO-deprotonation			NH-deprotonation	
	n	$\log\beta'_n$	$\log\beta'_n$/#HO	*n*	$\log\beta''_2$	*n*	$\log\beta'_n$	$\log\beta'_n$/#HO	*n*	$\log\beta''_2$
(*t*BuPh)$_4$PH$_2$ **1**	—	—	—	2.0	7.0	—	—	—	a	a
(HOPh)(*t*BuPh)$_3$PH$_2$ **2**	1.0	3.9	3.9	2.0	6.7	1.0	4.4	4.4	2.0	7.9
cis-(HOPh)$_2$(*t*BuPh)$_2$PH$_2$ **3**	2.0	7.0	3.5	2.0	5.9	2.0	9.0	4.5	2.0	7.1
trans-(HOPh)$_2$(*t*BuPh)$_2$PH$_2$ **4**	2.0	7.7	3.85	2.0	5.3	2.0	9.4	4.7	2.0	6.8
(HOPh)$_3$(*t*BuPh)PH$_2$ **5**	3.0	10.6	3.52	2.0	5.1	3.0	13.6	4.52	2.0	6.2
(HOPh)$_4$PH$_2$ **6**	4.0	13.3	3.32	2.0	5.0	4.0	17.3	4.32	2.0	6.1
Average value of $\log\beta'$			3.62 ± 0.25					4.49 ± 0.14		

[a] No data obtained due to the low solubility of the compound under the given solution conditions.

reaction is shown in Equation 2 and the calculated value of $\log\beta_2'' = 7.0$.

$$(t\text{BuPh})_4\text{PH}_2 + 2\text{OH}^- \rightleftharpoons [(t\text{BuPh})_4\text{P}]^{2-} + 2\text{H}_2\text{O} \quad (2)$$

In contrast to compound **1**, two sets of well-defined spectral changes were obtained during the titration of **2–6** with NaOH in DMF and DMSO. As examples the spectral changes of these compounds during the base titration were illustrated in Figs 6 and 7. Similar spectral changes were seen when the DMF was utilized as a solvent during the titration of a same compound. The spectral changes of compound **6** were also similar to that of previously reported in the literature [32] for the same compound. The Hill plots show a slope of 1.0 to 4.0 for the first step of the deprotonation where the experimentally observed value of *n* corresponds to the number of phenol HO groups on the porphyrin. The slope of the Hill plot in the second step ranges from 2.0 to 2.1 and involves deprotonation of the central nitrogen protons. This result indicates that all of the phenol groups on **2–6** are initially deprotonated in a simultaneous process involving 1–4 non-interacting HO

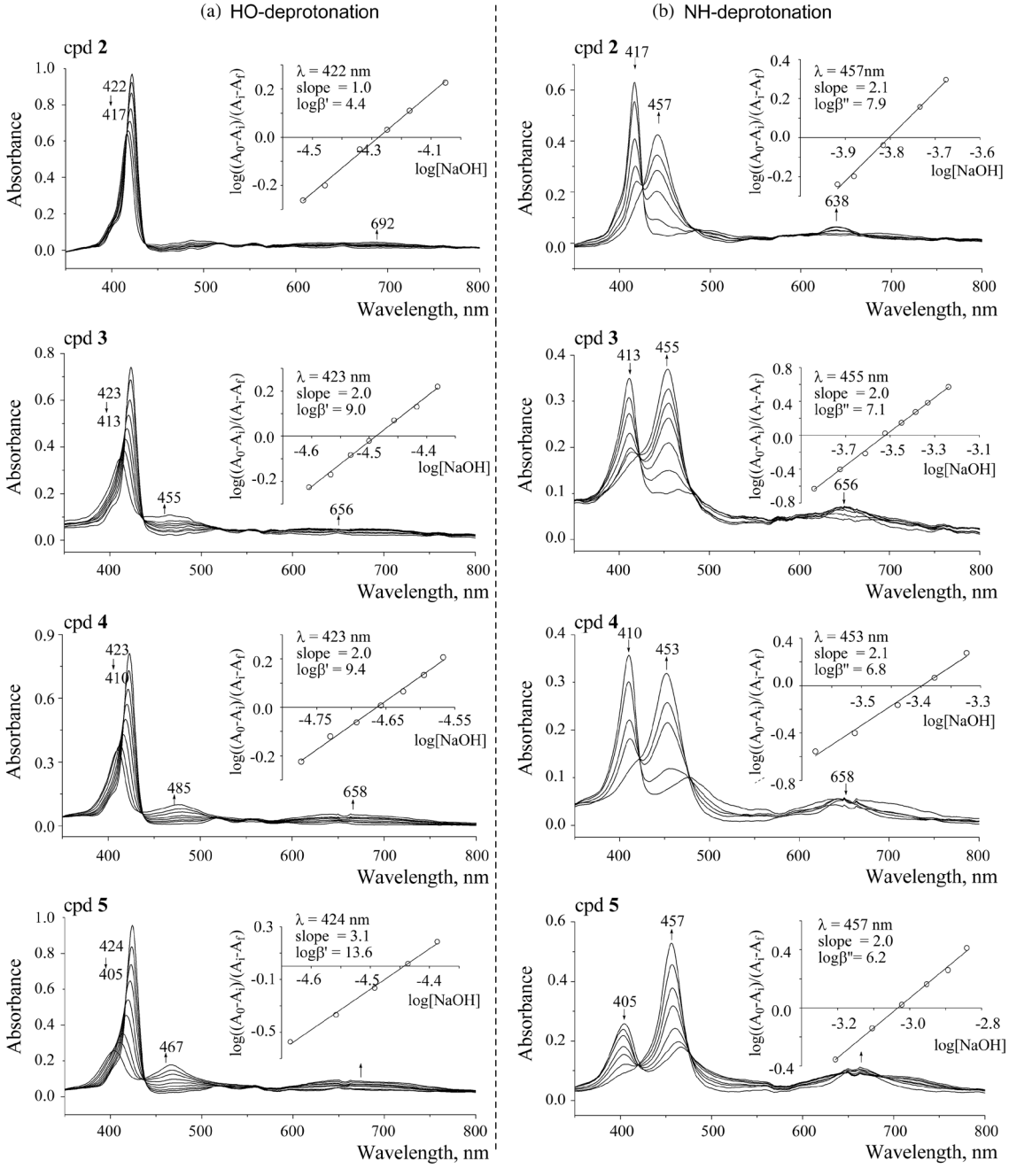

Fig. 6. UV-visible spectral changes during (a) HO-deprotonation and (b) NH-deprotonation of the phenol substituted free-base porphyrins **2–5** by addition of NaOH in DMSO. The inset shows the Hill plots used for calculation of the $\log\beta_n'$

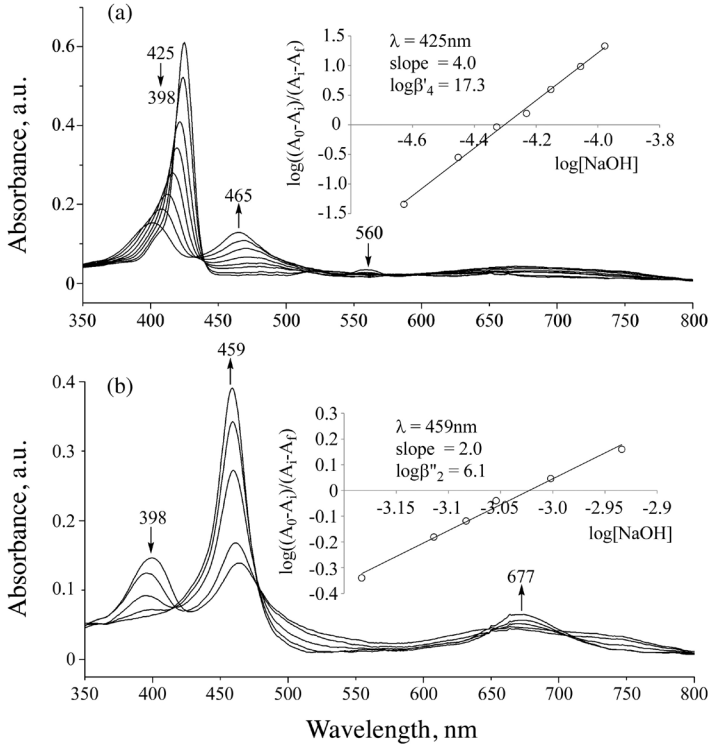

Fig. 7. UV-visible spectral changes of $(HOPh)_4PH_2$ **6** in DMSO during (a) the first and (b) second protonation steps with addition of NaOH solutions. The insert shows the Hill plot used for calculation of the $\log\beta'_4$ and $\log\beta''_2$

substituents followed by a simultaneous deprotonation of the two central NH protons as shown in Equations 3 and 4 as well as Scheme 2.

$$(HOPh)_n(t\text{BuPh})_{4-n}PH_2 + nOH^- \rightleftharpoons [(OPh)_n(t\text{BuPh})_{4-n}PH_2]^{n-} + nH_2O \quad (3)$$

$$[(OPh)_n(t\text{BuPh})_{4-n}PH_2]^{n-} + 2OH^- \rightleftharpoons [(OPh)_n(t\text{BuPh})_{4-n}P]^{(n+2)-} + (n+2)H_2O \quad (4)$$

Effect of HO substituents on the neutral spectra

Figure 8 plots the energy of the Soret band (*E*) for the investigated porphyrins in DCM, DMF or DMSO *vs.* the number of HO groups on the *meso*-phenyl rings of the macrocycle. A linear relationship is seen in DMF and DMSO where the energy systematically shifts towards lower values with increase of the number, but not the position of the phenol substituents. The fact that almost identical UV-visible spectra are obtained for *cis*-$(HOPh)_2(t\text{BuPh})_2PH_2$ **3** and *trans*-$(HOPh)_2(t\text{BuPh})_2PH_2$ **4** in all three solvents (see λ_{max} values in Table 3), indicates that the position of the two phenol substituents has no effect on the spectral properties of these compounds. The linear relationship between the number of HO substituents on the compounds and the energy of the porphyrin Soret band in DMSO and DMF contrasts with what occurs in DCM where increasing the number of phenol substituents from zero to four has no effect on the UV-visible spectra in this solvent. The phenyl HO groups are expected to hydrogen bond with the DMSO and DMF solvents and this solvent-porphyrin interaction would be increased as the number of HO groups on the molecule increases from 1 to 4. In contrast, little to no solvent interaction would be expected between DCM solvent and the phenol HO groups. Under these conditions, almost the same UV-vis spectrum might be expected for the six investigated compounds in this solvent, and this is indeed the case.

Effect of HO substituents on protonation/ deprotonation reactions

Shown in Fig. 9 are plots of the measured protonation reaction constants ($\log\beta_2$) in DCM, DMF and DMSO *vs.* the number of HO groups on the porphyrin. As seen from this figure, the value of $\log\beta_2$ for protonation at the central nitrogens of the porphyrins gradually increases upon going from compound **1** to **6** in both DMF and DMSO but a different trend is again observed in DCM, where $\log\beta_2$ decreases slightly with increase in the number of HO groups. Based only on the fact that HO is an electron-donating substituent [33] one might expect an increase in $\log\beta_2$ in all three solvents but this is not observed and, in fact, the substituent effect of the added HO groups on $\log\beta_2$ is close to negligible.

Plots of the measured deprotonation constants for the 1–4 protons of the phenol groups and the two protons

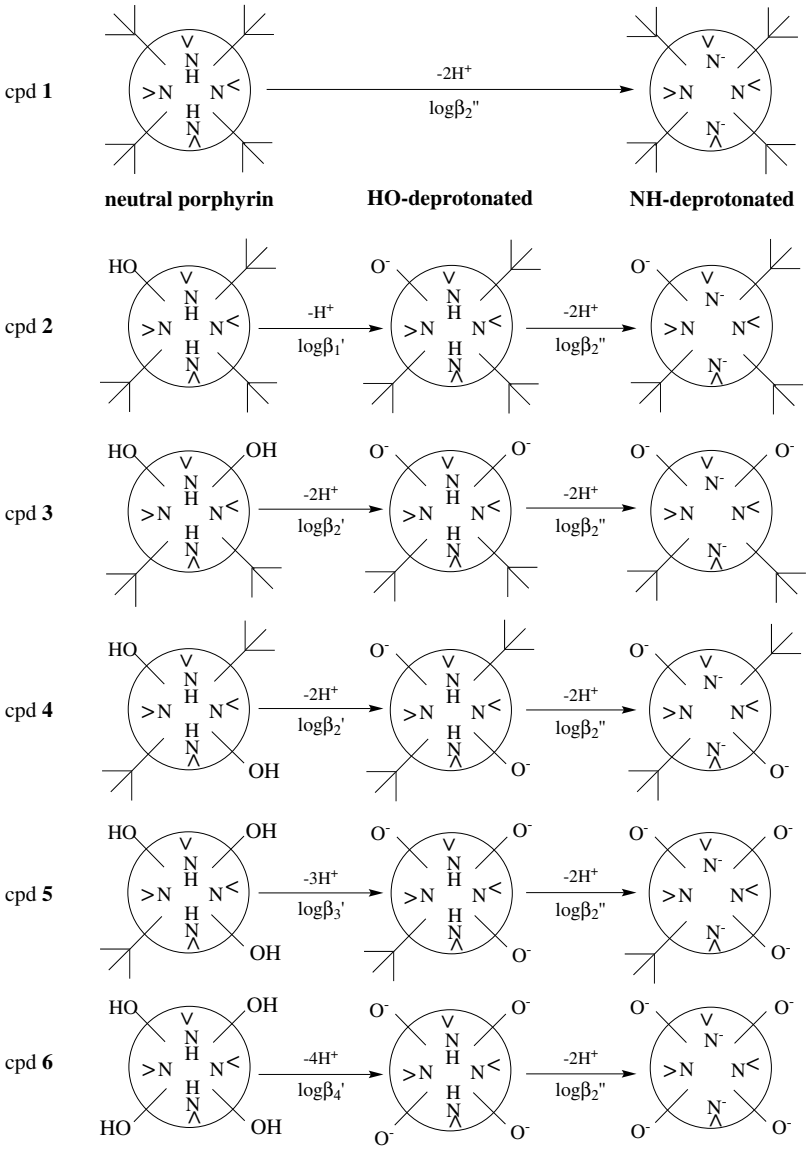

Scheme 2. Deprotonation reaction mechanisms of the porphyrins in DMF and DMSO with added NaOH solutions

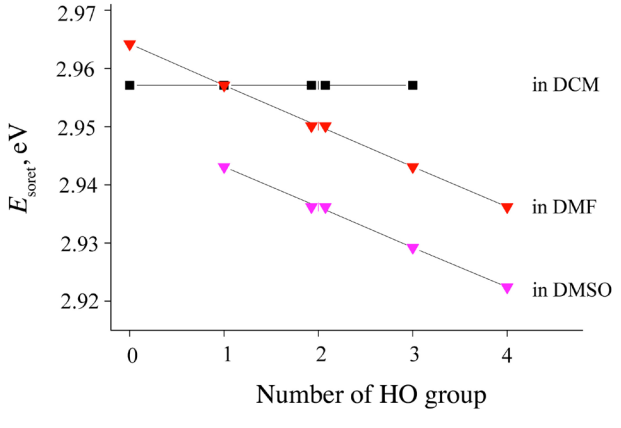

Fig. 8. Plots of the energy (eV) of the Soret band *vs.* the number of hydroxyl groups on the four *meso* phenyl rings of the porphyrin macrocycle. The values of λ_{max} for the Soret band of each compound is given in Table 3

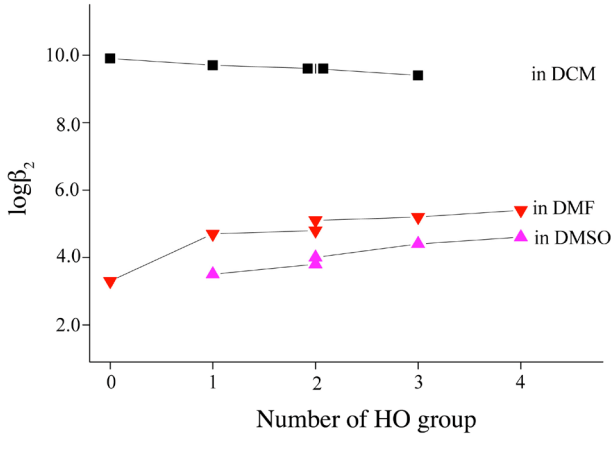

Fig. 9. Plots of the protonation reaction constants ($\log\beta_2$) *vs.* the number of hydroxyl groups on the four *meso* phenyl rings of the porphyrin macrocycle

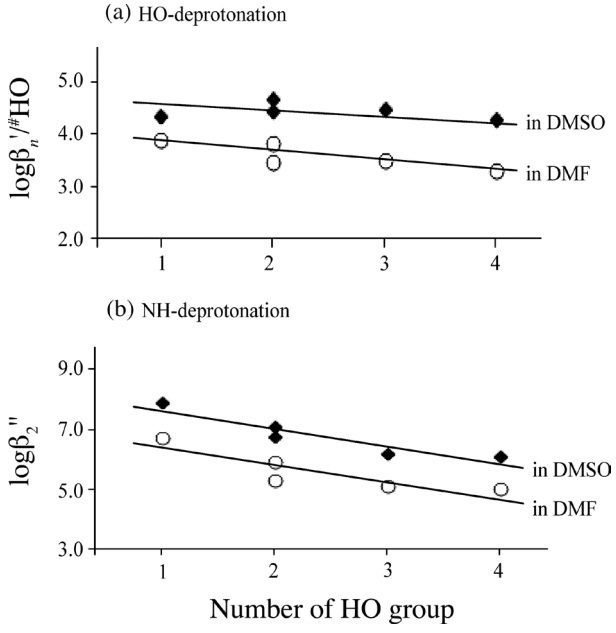

Fig. 10. Plots of the HO- and NH-deprotonation constants ($\log\beta'_n$ and $\log\beta''_2$) *vs.* the number of hydroxyl groups on the four phenyl rings of the macrocycle

of the porphyrin central nitrogens in compounds **2–6** are illustrated in Fig. 10. In order to better understand the trend in logβ′ for deprotonation of the phenol protons on $(HOPh)_n(t\text{BuPh})_{4-n}PH_2$, we have plotted in Fig. 10a the magnitude of logβ′ divided by the number of HO groups. This value is given in Table 5 as logβ′/#HO and is justified on the basis of the fact that all of the phenol deprotonations occur in a single overlapping step involving 1–4 HO groups depending on the specific compound. Under these conditions, all of the hydroxyl porphyrins have the same individual logβ′ values. When examing the average deprotonation constants for **2–6** it can be seen that the logβ′ values for deprotonation of the phenol HO groups are higher in DMSO than in DMF, and in both solvents, there is a slight decrease of logβ′ with increase in the number of HO groups. The average logβ′ for the five hydroxylated porphyrins is 3.62 in DMF and 4.48 in DMSO (Table 5).

Similar to what is observed for deprotonation of the phenol protons, the values of $\log\beta''_2$ for the NH-deprotonation also decrease with increasing number of phenol groups on the compound. Again the experimentally measured values are higher in DMSO than in DMF (see Fig. 10b). For example, the measured $\log\beta''_2$ decreases from 7.9 for $(HOPh)(t\text{BuPh})_3PH_2$ **2** to 6.1 for $(HOPh)_4PH_2$ **6** in DMSO (Table 5) and a similar decrease is seen for the same two porphyrins in DMF where $\log\beta''_2$ decreases from 6.7 for **2** to 5.0 for **6** (see Table 5). One reason that the NH protons of porphyrin **2** are easier to be deprotonated than those of **6** might be because compound **2** has a single negative charge after titration of the one phenol proton on the mono-hydroxyl derivative while compound **6** contains four negative charges after deprotonation of all four phenol protons and formation of $[(OPh)_4PH_2]^{4-}$.

CONCLUSION

In summary, we have synthesized a series of *meso* phenol substituted free-base porphyrins and determined the protonation and deprotonation constants of these compounds in three nonaqueous solvents. Each free-base porphyrin was doubly protonated in a single step by addition of TFA, leading to formation of $[(HOPh)_n(t\text{BuPh})_{4-n}PH_4]^{2+}$ in all three solvents. The *meso*-phenol and central nitrogen protons of the free-base porphyrins were also deprotonated by titration with NaOH in DMF and DMSO solutions. The *meso*-phenol protons are easier to deprotonate than the two protons at the central nitrogen atoms of the porphyrin and deprotonation of the hydroxyl group occurs as the first step in a titration of the porphyrin with NaOH.

Acknowledgements

We gratefully acknowledge supports from the Natural Science Foundation of China (No. 21071067, 21001054), Postdoctoral Science Foundation of China (2012M511203) and Jiangsu Province (1102126C), and the Robert A. Welch Foundation (K.M.K., Grant E-680).

Supporting information

Stereoview of the interlinked supramolecular organization for compound **4** and UV-visible spectral changes during protonation of free-base porphyrins **1**, **3–6** by addition of TFA in DMF (Figs S1 and S2) are given in the supplementary material. This material is available free of charge *via* the Internet at http://www.worldscinet.com/jpp/jpp.shtml.

Crystallographic data for **1** and **4** have been deposited at the Cambridge Crystallographic Data Centre (CCDC) under numbers CCDC-829498 and 827924. Copies can be obtained on request, free of charge, *via* www.ccdc.cam.ac.uk/data_request/cif or from the Cambridge Crystallographic Data Centre, 12 Union Road, Cambridge CB2 1EZ, UK (fax: +44 1223-336-033 or email: deposit@ccdc.cam.ac.uk).

REFERENCES

1. Hambright P. In *The Porphyrin Handbook*, Vol. 3, Kadish KM, Smith KM and Guilard R. (Eds.) Academic Press: Boston, 2000; pp 129–210.
2. Inisan C, Saillard JY, Guilard R, Tabard A and Mest YL. *New J. Chem.* 1998; 823–830.
3. Kadish KM, Van Caembelbecke E and Royal G. In *The Porphyrin Handbook*, Vol. 8, Kadish KM, Smith KM and Guilard R. (Eds.) Academic Press: San Diego, 2000; pp 1–114.

4. Kadish KM, Ou Z, Zhan R, Khoury T, E W and Crossley MJ. *J Porphyrins Phthalocyanines* 2010; **14**: 866–876.
5. Chiu KY, Tu YJ, Lee CJ, Yang TF, Lai LL, Chao I and Su YO. *Electrochimica Acta* 2012; **62**: 51–62.
6. Fukuzumi S, Ohkubo K, Imahori H, Shao J, Ou Z, Zheng G, Chen Y, Pandey RK, Fujitsuka M, Ito O and Kadish KM. *J. Am. Chem. Soc.* 2001; **123**: 10676–10683.
7. Pandey RK and Zheng G. In *The Porphyrin Handbook*, Vol. 6, Kadish KM, Smith KM and Guilard R. (Eds.) Academic Press: San Diego, 2000; pp 157–230.
8. Thomas AP, Saneesh Babu PS, Asha Nair S, Ramakrishnan S, Ramaiah D, Chandrashekar TK, Srinivasan A and Radhakrishna Pillai M. *J. Med. Chem.* 2012; **55**: 5110–5120.
9. Hsu CY, Nieh MP and Lai PS. *Chem. Commun.* 2012; **48**: 9343–9345.
10. Ethirajan M, Chen Y, Joshi P and Pandey RK. *Chem. Soc. Rev.* 2011; **40**: 340–362.
11. Ojadi ECA, Linschitz H, Gouterman M, Walter RI, Lindsey JS, Wagner RW, Droupadi PR and Wang W. *J. Phys. Chem.* 1993; **97**: 13192–13197.
12. Okada S and Segawa H. *J. Am. Chem. Soc*. 2003; **125**: 2792–2796.
13. Pasternack RF, Huber PR, Boyd P, Engasser G, Francesconi L, Gibbs E, Fasella P, Cerio Venturo G and Hinds L. *J. Am. Chem. Soc.* 1972; **94**: 4511–4517.
14. Aronoff S. *J. Phys. Chem.* 1958; **62**: 428–431.
15. Finikova O, Galkin A, Rozhkov V, Cordero M, Hägerhäll C and Vinogradov S. *J. Am. Chem. Soc.* 2003; **125**: 4882–4893.
16. Zhang Y, Li M, Lü M, Yang R, Liu F and Li K. *J. Phys. Chem. A.* 2005; **109**: 7442–7448.
17. Gonçalves PJ, De Boni L, Barbosa Neto NM, Rodrigues Jr JJ, Zílio SC and Borissevitch IE. *Chem. Phys. Lett.* 2005; **407**: 236–241.
18. Sun H and Ou Z. *J. Anal. Sci.* 2008; **24**: 356–358.
19. Ou Z, Sun H, Zhu W, Da Z and Kadish KM. *J. Porphyrins Phthalocyanines* 2008; **12**: 1–10.
20. Ou Z, Shen J, Shao J, E W, Galezowski M, Gryko DT and Kadish KM. *Inorg. Chem.* 2007; **46**: 2775–2786.
21. Lin W, Fang Y, Lv A, Li M, Lu G and Ou Z. *Li Hua Jian Yan Part B: Chem. Anal.* 2012; **4**: 381–383.
22. Senge M. *Photodiag. Photodyn. Ther.* 2012; **9**: 170–179.
23. Sakthitharan S, Christine E and Ross WB. *Tetrahedron* 2000; **56**: 1025–1046.
24. Adler AD, Longo FR, Finarelli JD, Goldmacher J, Assour J and Korsakoff L. *J. Org. Chem.* 1967; **32**: 476–476.
25. Van Esch J, Feiters MC, Peters AM and Nolte RJM. *J. Phys. Chem.* 1994; **98**: 5541–5551.
26. Shen J, Ou Z, Shao J, Galezowski M, Gryko DT and Kadish KM. *J. Porphyrins Phthalocyanines* 2007; **11**: 269–276.
27. Ellis PE, Linard JE, Szymanski T, Jones RD, Budge JR and Basolo F. *J. Am. Chem. Soc.* 1980; **102**: 1889–1896.
28. Littler BJ, Ciringh Y and Lindsey JS. *J. Org. Chem.* 1999; **64**: 2864–2872.
29. Hill JP, Wakayama Y, Akada M and Ariga K. *J. Phys. Chem. C.* 2007; **111**: 16174–16180.
30. Guo H, Jiang J, Shi Y, Wang Y, Liu J and Dong S. *J. Phys. Chem. B.* 2004; **108**: 10185–10191.
31. Meat-Ner M and Adler AD *J. Am. Chem. Soc.* 1975; **97**: 5107–5111.
32. Guo H, Jiang J, Shi Y, Wang Y, Wang Y and Dong S. *J. Phys. Chem. B.* 2006; **110**: 587–594.
33. Zuman P. *Substituent Effect in Organic Polarography*, Plenum Press: New York, 1967.